atmosphere

MDPI

Article

Wet Deposition Characteristics of Inorganic Elements in Typical Chinese Coastal Cities

Zhengni Li [1], Dan Li [2,*], Hang Xiao [3,4,*], Chunli Liu [5] and Cenyan Huang [1,*]

[1] College of Biological and Environmental Sciences, Zhejiang Wanli University, Ningbo 315100, China
[2] Environmental Protection Monitoring Station of Shengzhou, Shaoxing 312400, China
[3] Center for Excellence in Regional Atmospheric Environment & Fujian Key Laboratory of Atmospheric Ozone Pollution Prevention & Key Laboratory of Urban Environment and Health, Institute of Urban Environment, Chinese Academy of Sciences, Xiamen 361021, China
[4] Zhejiang Key Laboratory of Pollution Control for Port-Petrochemical Industry & Ningbo Key Laboratory of Urban Environmental Pollution and Control, CAS Haixi Industrial Technology Innovation Center in Beilun, Ningbo 315830, China
[5] Yunnan Guoke Green Environmental Protection Co., Ltd., Kunming 650206, China
* Correspondence: lidan00310@126.com (D.L.); hxiao@iue.ac.cn (H.X.); cyhuang@zwu.edu.cn (C.H.)

Abstract

During wet deposition, particulate matter and gaseous species in the atmosphere are ultimately transported to the Earth's surface via precipitation and subsequently incorporated into terrestrial ecosystems. Therefore, investigating the fluxes, chemical compositions, and source apportionment of regional wet deposition is of great scientific importance. An analysis of the concentrations, deposition fluxes, spatiotemporal variations, and source apportionment of water-soluble ions in wet deposition can further enhance our understanding of the water-soluble ion characteristics, atmospheric pollution profiles, and potential ecosystem impacts of wet deposition in the Yangtze River Delta and Pearl River Delta regions. Coastal cities in China are most developed regions, and also areas suffering from severe air pollution. This study investigates the chemical characteristics, sources and wet deposition fluxes of water-soluble inorganic ions in precipitation in two typical coastal urban agglomerations of China: Ningbo in the Yangtze River Delta and Guangzhou in the Pearl River Delta. Precipitation samples were collected and analyzed to determine the concentrations of major ions. The results revealed distinct ionic compositions between the two regions. In Ningbo, NO_3^- and SO_4^{2-} were the predominant ions accounting for 16.98% to 23.22% of the total, reflecting the influence of anthropogenic emissions from fossil fuel combustion and mobile sources with the NO_3^-/SO_4^{2-} ratio of 0.90 and 0.70. In Guangzhou, precipitation was characterized by high contributions of SO_4^{2-}, NO_3^-, NH_4^+, and Ca^{2+}, accounting for 17.22% to 23.29% of the total, indicating a mixed influence of industrial emissions, agricultural activities, and construction dust with the NO_3^-/SO_4^{2-} ratio of 0.92 and 0.87. A clear inverse relationship between rainfall amount and ion concentration was observed at all sites ($p < 0.05$), demonstrating a significant dilution effect. Seasonality played a crucial role in deposition fluxes. In Ningbo, fluxes peaked during summer from 4667 to 5156 $mg \cdot m^{-2}$, while in Guangzhou, distinct dry and rainy season patterns influenced the scavenging efficiency of different ion species. Urban sites exhibited enhanced scavenging of crustal and anthropogenic ions (e.g., Ca^{2+}, NH_4^+) during the rainy season, whereas the coastal site showed elevated fluxes of marine-derived ions (Na^+, Cl^-, Mg^{2+}, SO_4^{2-}) during the same period. The observed trends in ion fluxes suggest a gradual improvement in regional air quality over the study period. These findings elucidate the complex interactions between anthropogenic activities, natural sources, and meteorological factors in shaping the wet deposition chemistry in coastal urban environments, providing

Academic Editor: Hung-Lung Chiang

Received: 24 March 2026
Revised: 7 May 2026
Accepted: 9 May 2026
Published: 13 May 2026

essential data for developing regional deposition models and assessing the ecological impacts of atmospheric pollution.

Keywords: atmospheric wet deposition; water-soluble inorganic ions; wet deposition fluxes; coastal cities

1. Introduction

When gaseous and particulate pollutants are released into the atmosphere via emission sources, they are subsequently removed through a series of scavenging mechanisms. This removal process is a form of atmospheric self-cleansing and essential for maintaining a relatively balanced atmospheric composition [1]. Among these mechanisms, wet deposition is a primary form of atmospheric self-purification because it effectively reduces long-term pollutant levels in the air [2]. During wet deposition, natural precipitation (rain, snow, hail, etc.) dissolves or suspends atmospheric particles and gases in water or ice, which are then brought to the Earth's surface by rainfall and enter terrestrial ecosystems [3]. As the most significant pathway through which atmospheric pollutants are delivered to ecosystems, wet deposition not only reflects the self-cleansing capacity of the atmosphere but also facilitates the transfer of various pollutants to surface environments. These deposited pollutants exert continuous influences on both terrestrial and aquatic ecosystems, directly or indirectly affecting biogeochemical cycles such as those of nitrogen and sulfur [4,5]. Furthermore, they contribute to regional and even global atmospheric pollution, potentially impacting climate systems and, consequently, human health [6,7]. Therefore, investigating the fluxes, chemical compositions, and sources of regional wet deposition is of great scientific importance. Such research provides critical insights into the mechanisms, current status, and ecological effects of regional air pollution, thereby holding substantial practical significance for advancing the understanding of atmospheric processes and their environmental implications.

The ionic components in rainwater primarily include Na^+, Ca^{2+}, Mg^{2+}, NH_4^+, K^+, Cl^-, SO_4^{2-}, NO_3^-, and F^-. During haze episodes, additional ions such as Al^{3+}, Ba^{2+}, and Fe^{3+} have also been detected [8]. Emissions of atmospheric pollutants such as nitrogen oxides (NO_x) and sulfur dioxide (SO_2) in the Central, Southwestern, Southern, and Eastern China are closely linked to regional anthropogenic activities. These include coal combustion for energy, industrial development, and the rapid increase in motor vehicle usage [9]. NO_x and SO_2 can be readily converted into nitric acid and sulfuric acid, respectively, through dissolution in atmospheric water [10,11]. In addition, construction dust and agricultural fertilization significantly influence the ionic concentrations in rainfall [12,13]. In coastal or island regions, inorganic pollutants in precipitation originate from a combination of regional crustal dust, anthropogenic emissions and long-range transport of marine-derived sulfates and nitrates [14].

Globally, the chemical characterization of atmospheric wet deposition is a key environmental research focus, driven by the need to understand biogeochemical cycles and transboundary pollutant transport. Countries including the United States and South Africa have established long-term monitoring networks [15,16]. China, which has been identified as a major contributor to global reactive nitrogen emissions and a hotspot for sulfur and trace metal deposition [17,18], has established extensive observational networks to quantify wet deposition fluxes. These studies have highlighted the pronounced spatial heterogeneity across Chinese terrestrial ecosystems, where multi-elemental stoichiometric ratios of wet deposition deviate significantly from ecosystem requirements, potentially exacerbating nutrient imbalances and ecological stress [17]. Furthermore, the interaction between precipitation events and aerosol loading has been shown to govern the scavenging efficiency of

fine particulate matter, a process that is particularly critical in the densely populated and industrialized coastal regions of China [19]. In the Pearl River Delta specifically, studies have identified that wet deposition fluxes of toxic elements are not only high compared to global background levels but are also predominantly sourced from long-range transport pathways and industrial emissions originating outside the immediate metropolitan area [18]. Despite these advances, there remains a need for more integrated and comparative assessments of inorganic wet deposition across China's major urban agglomerations, particularly between the Yangtze River Delta and the Pearl River Delta, to better constrain regional emission influences and deposition prediction models.

The Yangtze River Delta and the Pearl River Delta are among the most economically dynamic and developed regions in China. They are characterized by high population density, advanced industrialization and high levels of urbanization. With rapid economic growth, atmospheric pollution in these regions has drawn considerable attention from both government authorities and the academic community. In recent years, comprehensive air pollution control measures have been continuously implemented. Focusing primarily on water-soluble ions, this study selected two representative sampling sites (urban and coastal sites) in each of the two cities, Ningbo and Guangzhou, as the representative cities in the Yangtze River Delta and the Pearl River Delta, respectively. Based on observations of water-soluble ions in precipitation in the typical cities of Guangzhou and Ningbo, this study analyzed the concentrations, spatiotemporal variations, and sources of these ions, and further investigated the chemical characteristics of atmospheric precipitation in the two regions. The results provide valuable guidance for understanding the actual status of inorganic element deposition in the two economically developed regions of the Yangtze River Delta and Pearl River Delta. This research aims to provide critical data for the development of wet deposition flux prediction models. Ultimately, the findings will support the extension of wet deposition flux prediction to broader regional scales.

2. Materials and Methods

2.1. Study Sites

The field study was carried out in two cities in China shown in Figure 1. Ningbo is located in the eastern coastal region of China, situated in the central section of the mainland coastline and forming the southern wing of the Yangtze River Delta. Ningbo experiences a typical subtropical monsoon climate, characterized by mild, humid and rainy conditions with distinct seasons. The multi-year average temperature is 16 °C and the average annual rainfall is approximately 1480 mm. The Zhangxi (ZX) sampling site (29.80° N, 121.33° E) is located in Zhangshui Town, Haishu District, approximately 20 km from the main urban area. This site is adjacent to a dense transportation network. The Ningbo Urban Environment Observation and Research Station of the Chinese Academy of Sciences (CX) sampling site (29.75° N, 121.75° E) is situated in Chunxiao Town, Beilun District. This site borders the East China Sea within 1 km and is surrounded by industrial parks.

Guangzhou, a core city in the Pearl River Delta region, is located in southern China. Guangzhou has a typical subtropical maritime monsoon climate, characterized by warm, humid and rainy conditions with abundant sunshine. The annual average temperature is 21 °C, and the average relative humidity is 77%, and the annual rainfall is approximately 1720 mm. The Guangzhou Institute of Geochemistry, Chinese Academy of Sciences (GIG) sampling site (23.12° N, 113.36° E) is located in Tianhe District, an area characterized by a dense traffic network and high traffic volume. The Wanqingsha (WQS) sampling site (22.71° N, 113.55° E) is situated at in Wanqingsha Town, Nansha District. This site serves as an important port and logistics industrial base and is approximately 52 km from the urban area.

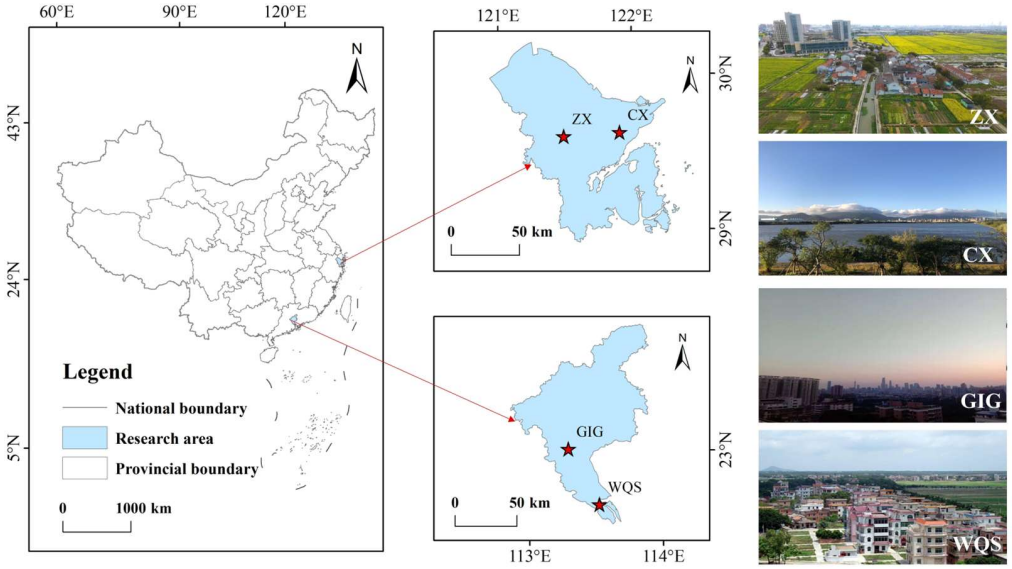

Figure 1. Geographical locations of sampling area.

2.2. Samples Collection

Wet deposition samples were collected using automated wet depoition samplers (ZR-3901, Qingdao Zhongrui, China and APS-3A, Changsha, China). These samplers are designed to automatically initiate sample collection at the onset of a rainfall event and to collect wet deposition continuously throughout the entire duration of the rainfall period. Only periodic sample retrieval by field personnel was required according to the experimental protocol. In this study, wet deposition samples were collected at the urban site (ZX) and the coastal site (CX) in Ningbo from January 2018 to December 2020. Samples were also collected at the urban site (GIG) and the coastal site (WQS) in Guangzhou from September 2016 to August 2019 (Figure S1). A total of 87 valid wet deposition samples were obtained during the study period.

The frequency of sample retrieval was determined based on the regional rainfall frequency and amount. During the rainy seasons of spring and summer, samples were retrieved every five days. During autumn and winter, when rainfall was less frequent, retrieval was conducted every fifteen days. Following each retrieval, the sampling containers were rinsed with ultrapure water to prevent cross-contamination between successive samples. All samples were stored in Teflon bottles. Prior to use, each Teflon bottle was subjected to a rigorous cleaning protocol: bottles were first soaked for seven days in a 1:1:1 mixture of dichloromethane, methanol, and n-hexane, followed by an additional seven days of soaking in 10% nitric acid to eliminate potential trace metal contamination. Finally, the bottles were thoroughly rinsed with ultrapure water, dried, and stored until deployment. Collected samples were immediately preserved in a freezer at −20 °C pending analysis. Sample analysis was completed within one month after collection.

2.3. Samples Analysis

Sample analysis was conducted following the USEPA method [20]. A 9 mL aliquot of each sample was placed into a Teflon digestion vessel, followed by the addition of 5 mL of concentrated HNO_3 and 2 mL of concentrated HF. Digestion was performed using a microwave digestion system (XT-9912, Xintuo, Suzhou, China) at 170 °C for 2 h. After the instrument had cooled to room temperature, the digestion vessels were removed and transferred to a sample pretreatment heating apparatus (XT-9816-II, Xintuo, Shanghai, China) for acid evaporation at 120 °C for 2 h. Subsequent to evaporation, 1 mL of concentrated HNO_3 was added to the digested solution, which was then diluted to a final volume of 10 mL

prior to analysis. Blank samples were prepared with ultrapure water and subjected to the same pretreatment and digestion procedures as the samples. The digested solutions were analyzed using an inductively coupled plasma mass spectrometer (ICP-MS, Thermo Fisher, Waltham, MA, USA) for the determination of trace metal elements. The calibration curve was plotted using the external standard method, with the linear correlation coefficient ensured to be above 0.999. For each batch of sample analysis, the laboratory reagent blank and the field blank were simultaneously determined. When the concentration of the analyte in the sample exceeded the range of the calibration curve, the sample was diluted and re-measured. All sample preparation procedures were conducted on a Class-100 clean bench to prevent contamination.

Ion chromatography (IC) was performed for the determination of water-soluble ions (NH_4^+, Na^+, K^+, Mg^{2+}, Ca^{2+}, SO_4^{2-}, NO_3^-, Cl^-, and F^-). Two ion chromatographs were utilized: a Metrohm system (833 Basic IC plus, Metrohm, Herisau, Switzerland) and a Thermo Fisher system (ICS-5000, Thermo Fisher, Waltham, MA, USA). For the Metrohm system, anion separation was achieved using a Metrosep A Supp 4250/4.0 column with a Metrosep A Supp 4/5 Guard pre-column, while cation analysis employed a Metrosep C 4100/4.0 column with a Metrosep C4 Guard pre-column. The anion eluent consisted of a mixed solution of 1.8 mmol·L^{-1} Na_2CO_3 and 1.7 mmol·L^{-1} $NaHCO_3$, prepared by dissolving 0.678 g of Na_2CO_3 and 0.168 g of $NaHCO_3$ (guaranteed reagent grade) in 2 L of ultrapure water, followed by vacuum filtration to remove dissolved gases. The cation eluent was 2 mmol·L^{-1} H_2SO_4, prepared by adding 0.22 mL of concentrated sulfuric acid to 2 L of ultrapure water and filtering. A suppressor solution of 50 mmol·L^{-1} H_2SO_4 and ultrapure water (18.2 MΩ·cm) was employed for suppression. For the Thermo Fisher system, an AS11 4 × 250 mm analytical column was used for anion analysis, and a CS12A 4 × 250 mm column was used for cation analysis.

Quality assurance and quality control procedures were rigorously implemented. Instrumental detection limits (IDLs) were determined as three times the standard deviation (SD) of seven consecutive injections of the lowest concentration standard divided by the slope of the calibration curve (3 × SD/k). Method detection limits (MDLs) were subsequently calculated based on the air sampling volume. The detection limits for all target ions were below 0.02 μg·mL^{-1}. Recovery was evaluated for both anions and cations by spiking known concentrations of standard solutions onto blank quartz fiber filters. The spiked filters were subjected to ultrasonic extraction and analyzed following the identical procedure used for environmental samples. Five replicate experiments were conducted in parallel, yielding recoveries for all target ions above 98%, with a relative standard deviation (RSD) of less than 5%. Across all sample analyses, overall recovery rates ranged from 80% to 110%, and the relative standard deviation was maintained below 5%.

2.4. Calculation of Water-Soluble Ionic Charge Balance

Previous studies have shown that the acidity or alkalinity of atmospheric particulate matter is primarily influenced by the water-soluble anions and cations present in the particles [21,22]. The molar charge ratio of water-soluble anions to cations (*CE*/*AE*) serves two purposes: first, it determines the pH value of atmospheric particulate matter; second, it can be used to assess the reliability of water-soluble ion data. Aqueous solutions must maintain electrical neutrality, meaning the total positive charge from cations equals the total negative charge from anions. If the molar charge ratio of anions to cations deviates from 1:1, the imbalance is compensated by H^+ or OH^- from water dissociation. A *CE*/*AE* value closer to 1 indicates more reliable data for water-soluble anions and cations. *AE* and

CE represent the charge concentrations of water-soluble anions and cations, respectively, and are calculated using the formulas shown below:

$$AE(Anion\ equivalent) = \frac{Cl^-}{35.5} + 2 \times \frac{SO_4^{2-}}{96} + \frac{NO_3^-}{62} \quad (1)$$

$$CE(Cation\ equivalent) = \frac{Na^+}{23} + 2 \times \frac{Mg^{2+}}{24} + 2 \times \frac{Ca^{2+}}{40} + \frac{NH_4^+}{18} + \frac{K^+}{39} \quad (2)$$

where *AE* denotes the anion equivalent concentration ($\mu eq \cdot L^{-1}$); *CE* denotes the cation equivalent concentration ($\mu eq \cdot L^{-1}$); the individual ion concentrations are expressed as mass concentrations ($\mu g \cdot L^{-1}$).

3. Results and Discussion

3.1. The Concentration Levels of Water-Soluble Ions in Atmospheric Wet Deposition

Figure 2 and Table S1 present statistical summaries, including mean values, standard deviations and coefficients of variation, for water-soluble ion concentrations in all rainfall samples collected at the ZX and CX sites in Ningbo from January 2018 to December 2020. At the ZX site, the water-soluble ion concentrations in rainfall samples ranked in descending order as follows: $SO_4^{2-} > NO_3^- > Ca^{2+} > NH_4^+ > Cl^- > Na^+ > Mg^{2+} > K^+ > F^-$. The predominant ions were SO_4^{2-} and NO_3^-, with concentrations of 68.02 $\mu eq \cdot L^{-1}$ and 60.67 $\mu eq \cdot L^{-1}$, respectively. At the CX site, the order was $SO_4^{2-} > NO_3^- > NH_4^+ > Cl^- > Ca^{2+} > Na^+ > Mg^{2+} > K^+ > F^-$, with NO_3^- and SO_4^{2-} concentrations of 41.09 $\mu eq \cdot L^{-1}$ and 58.76 $\mu eq \cdot L^{-1}$, respectively. Concentrations of Na^+ and Cl^- were lower in urban samples than in those from the coastal site, whereas all other ions exhibited higher concentrations in urban samples. This pattern may be attributed to the greater influence of sea salt at the coastal CX site due to its proximity to the ocean.

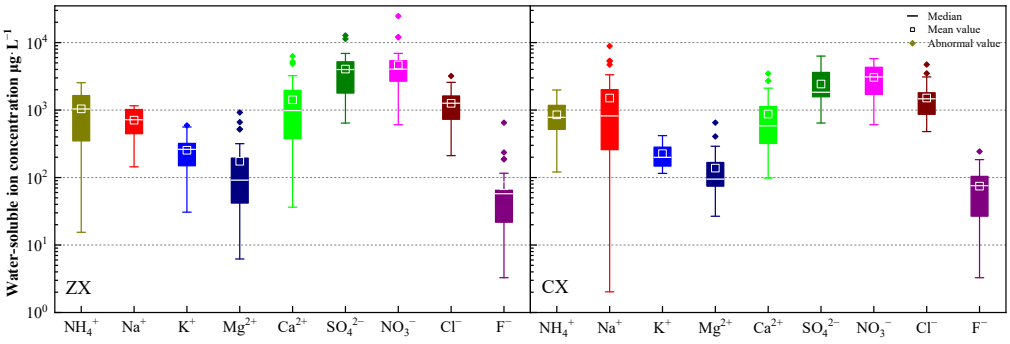

Figure 2. Statistical characteristics of Water-soluble ionic elements in wet deposition in Ningbo.

The dominant anions in Ningbo precipitation are NO_3^- and SO_4^{2-}, while the dominant cations are Ca^{2+} and NH_4^+. Statistical analysis revealed considerable differences in the coefficients of variation (CV) for water-soluble ion concentrations between the two sites. At the ZX site, K^+ exhibited the highest CV at 119%, while Na^+, Mg^{2+} and Ca^{2+} also showed CVs exceeding 100%, classifying them as highly variable ions. At the CX site, Mg^{2+} displayed the highest CV at 104%, representing the only ion with strong variability at this location. Ningbo is characterized by a typical maritime monsoon climate, with high precipitation in summer and lower rainfall in autumn and winter, contributing to substantial fluctuations in the chemical composition of precipitation.

Figure 3 and Table S2 present statistical summaries for water-soluble ions in all rainfall samples collected at the urban site (GIG) and the coastal site (WQS) in Guangzhou from September 2016 to August 2018. The results indicate that SO_4^{2-} and NO_3^- were the most abundant ions at both sites. At the GIG site, the concentrations of water-soluble ions ranked

in descending order as follows: SO_4^{2-} > NO_3^- > NH_4^+ > Ca^{2+} > Cl^- > Na^+ > Mg^{2+} > F^- > K^+, with SO_4^{2-} and NO_3^- concentrations of 117.03 μeq·L^{-1} and 107.67 μeq·L^{-1}, respectively. At the WQS site, the order was SO_4^{2-} > NH_4^+ > Ca^{2+} > NO_3^- > Cl^- > Na^+ > Mg^{2+} > F^- > K^+, with SO_4^{2-} and NO_3^- concentrations of 102.64 μeq·L^{-1} and 89.42 μeq·L^{-1}, respectively.

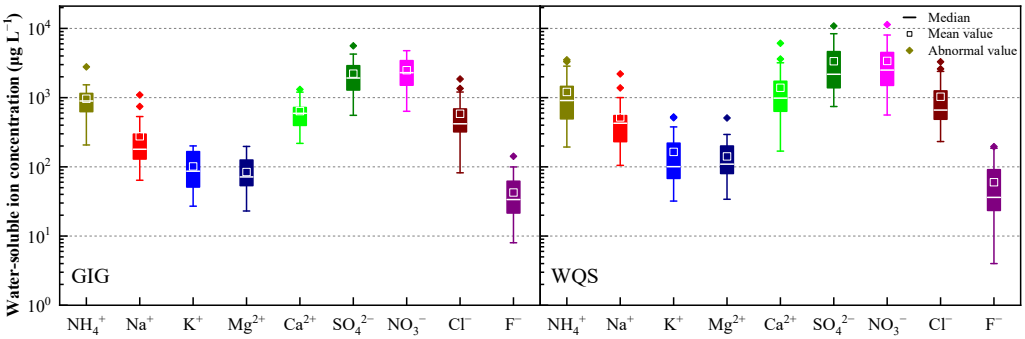

Figure 3. Statistical characteristics of water-soluble ionic elements in wet deposition in Guangzhou.

Concentrations of NH_4^+, SO_4^{2-}, NO_3^- and K^+ were slightly higher at GIG than at WQS, whereas Na^+, K^+, Mg^{2+}, Ca^{2+}, and Cl^- exhibited higher concentrations at WQS. Previous studies have demonstrated that SO_4^{2-}, NO_3^- and NH_4^+ originate predominantly from anthropogenic activities, representing major pollution sources. Na^+ and Cl^- are typically derived from marine sources, and Mg^{2+} and Ca^{2+} primarily originate from crustal dust sources [23]. Considerable variability was observed in ion concentrations at both sites. At GIG, NO_3^- and NH_4^+ exhibited the highest coefficients of variation at 88% and 86%, respectively, with no ions showing CVs exceeding 100%. At WQS, F^- displayed the highest CV at 102%, indicating strong variability. These findings suggest a relatively heterogeneous distribution of water-soluble ions in precipitation across the study period. This heterogeneity can be attributed primarily to substantial seasonal variations in rainfall amounts, which influenced ion concentrations in precipitation. In addition, the influence of surrounding environmental conditions at the sampling sites also impacted the sources and distribution patterns of water-soluble ions.

The results above indicate that significant differences exist in the water-soluble ion concentrations of rainwater samples collected from Ningbo and Guangzhou. The ion concentrations at urban and coastal sites exhibit distinct spatial characteristics corresponding to their geographical locations. Specifically, urban sites are characterized by higher NH_4^+ concentrations due to intensive urbanization and anthropogenic activities. In contrast, coastal sites show higher Na^+ and Cl^- levels compared to urban areas, suggesting that these two ions are strongly influenced by marine aerosols.

The concentrations of water-soluble ions in wet deposition samples vary considerably, which can be attributed to the combined effects of seasonal variations and heterogeneous surrounding environments, thereby reflecting the unique regional environmental properties. SO_4^{2-} and NO_3^- are the primary ions responsible for rainwater acidity. The ratio of SO_4^{2-} to NO_3^- can be used to preliminarily identify the acidity type of local rainwater: rainwater is classified as sulfate-type when the ratio is higher than 3, mixed-type when the ratio ranges from 0.5 to 3, and nitrate-type when the ratio is lower than 0.5 [24]. Both Ningbo and Guangzhou exhibit high concentrations of SO_4^{2-} and NO_3^-. The rainwater types were determined by calculating the SO_4^{2-}/NO_3^- ratios at four sampling sites ZX, CX, GIG and WGS in the two cities, which were 1.12, 0.94, 1.09, and 1.15, respectively. The results demonstrate that rainwater in both Ningbo and Guangzhou belongs to the sulfate-nitrate mixed type. Additionally, the acidic components in rainwater at ZX, GIG, and

WQS sites show that SO_4^{2-} concentrations are slightly higher than those of NO_3^-. These findings suggest that regional air pollution control in Ningbo and Guangzhou should target both sulfur dioxide and nitrogen oxide emissions simultaneously to effectively mitigate acid deposition.

3.2. Comparison of the Chemical Characteristics of Water-Soluble Ions in Other Cities in China

To better elucidate the chemical characteristics of water-soluble ions in wet deposition within the study areas, data from selected major cities in China were compared with the findings of this research (Table 1). Significant differences exist in the distribution of water-soluble ions in precipitation across various climatic and geographical regions of China. Northern cities (Beijing, Xi'an, Lanzhou), situated in the temperate semi-humid/semi-arid zone, are subject to the impacts of loess dust and coal combustion emissions in northern China. The concentrations of Ca^{2+}, SO_4^{2-} and NH_4^+ are notably higher, with precipitation being neutral to alkaline. These ions are primarily derived from crustal and industrial coal combustion sources; Ca^{2+} accounts for a prominent proportion in Lanzhou, whereas secondary inorganic ions dominate in Xi'an and Beijing. Cities in the middle and lower reaches of the Yangtze River and Southwest China (Nanjing, Wuhan, Chengdu, Chongqing) are located in the subtropical humid monsoon zone, where the overall ion concentrations are lower than those in northern China. Ca^{2+} and NH_4^+ remain the dominant cations. Due to long-term acid rain control measures in Chongqing, the proportion of SO_4^{2-} has decreased while that of NO_3^- has increased, leading to a transformation of acid rain type from sulfuric acid-dominated to a sulfuric-nitric acid mixed type. In Chengdu, ions exhibit a distinct seasonal pattern of higher concentrations in winter and lower in summer, while Wuhan is jointly influenced by industrial emissions and regional transport. Coastal cities (Xiamen, Qingdao, Ningbo, Guangzhou) are affected by land–sea interaction, resulting in significantly higher concentrations of Na^+ and Cl^- compared to inland areas, with sea salt sources making a prominent contribution. Additionally, superimposed with land-based anthropogenic pollution and dust input, the ion sources are characterized by the coexistence of marine sources, vehicle sources, coal combustion sources and dust sources [25].

Table 1. Comparison of water-soluble ion concentration in wet deposition in Chinese main cities ($\mu eq \cdot L^{-1}$).

Study City	NH_4^+	Na^+	K^+	Mg^{2+}	Ca^{2+}	SO_4^{2-}	NO_3^-	Cl^-	F^-
Beijing [26]	376.0	12.5	8.2	15.3	397.0	521.0	174.0	22.6	5.8
Xi'an [27]	229.8	31.1	13.8	36.6	425.6	489.7	128.8	38.7	28.7
Lanzhou [28]	45.2	18.5	7.3	22.1	886.0	215.3	77.2	25.4	3.1
Chengdu [29]	118.5	9.2	6.8	8.5	92.3	135.7	82.6	15.4	2.3
Chongqing [30]	98.7	15.6	5.9	7.8	76.5	124.3	95.8	22.1	1.9
Nanjing [31]	86.4	11.3	4.7	6.2	105.8	98.5	76.3	18.9	1.5
Wuhan [32]	72.3	14.8	5.1	7.4	89.6	85.7	68.2	20.5	1.7
Xiamen [33]	42.5	68.3	8.7	12.6	56.8	58.9	45.3	72.4	2.8
Qingdao [34]	38.6	85.2	7.9	15.3	62.4	52.7	39.8	88.6	2.5
Ningbo	40.27	22.83	5.86	10.81	39.03	63.39	50.88	33.12	4.37
Guangzhou	101.34	31.98	4.27	17.83	88.42	109.84	98.55	43.10	5.10

In general, ion concentrations and compositions are jointly regulated by climate aridity/humidity, crustal dust intensity, sea salt input, and anthropogenic emission structure. Regarding seasonal variations, northern regions exhibit greater seasonal differences due to the impacts of sand dust and heating activities, while seasonal distribution in southern regions is mostly dominated by meteorological wet scavenging processes.

3.3. The Composition Characteristics of Water-Soluble Ions in Atmospheric Wet Deposition

Figure 4 presents the percentage contributions of individual ions to total ionic concentration in wet deposition samples collected at four observation sites in Ningbo and Guangzhou. The dominant water-soluble ions at the ZX site were SO_4^{2-}, NO_3^-, and Ca^{2+}, accounting for 20.71%, 23.22%, and 15.61% of the total ionic concentration, respectively. At the CX site, the dominant ions were NO_3^-, SO_4^{2-}, and NH_4^+, contributing 18.00%, 16.98%, and 16.47%, respectively. Mg^{2+}, K^+ and F^- exhibited relatively low total percentage contributions, with their combined proportions reaching 8.31% at ZX and 7.77% at CX.

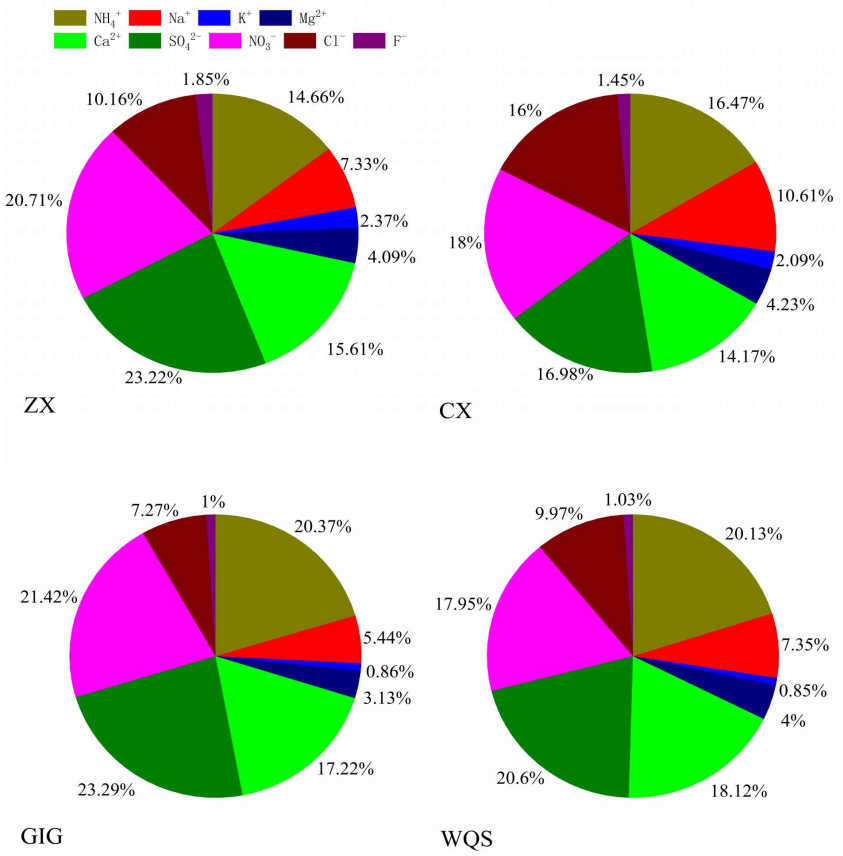

Figure 4. Percentage of each ion in the total ion concentration of the wet deposition sample.

At the Guangzhou sites, SO_4^{2-}, NO_3^-, NH_4^+ and Ca^{2+} were identified as the dominant water-soluble ions in wet deposition at both GIG and WQS. At GIG, these ions contributed 23.29%, 21.42%, 20.37%, and 17.22%, respectively, while at WQS their contributions were 20.60%, 17.95%, 20.13%, and 18.13%, respectively. Mg^{2+}, F^- and K^+ exhibited the lowest percentage contributions at both sites, with combined proportions of 4.99% at GIG and 5.89% at WQS.

The percentage contributions of Na^+ and Cl^- were higher at coastal sites than at urban sites in both Ningbo and Guangzhou. As coastal metropolises adjacent to the East China Sea (Ningbo) and South China Sea (Guangzhou), marine monsoons and coastal breezes transport sea salt aerosols to coastal areas, increasing Na^+ and Cl^- input in precipitation. In contrast, urban anthropogenic activities dilute sea salt-derived ions, lowering their relative contributions. NO_3^- in wet deposition is primarily formed through a series of chemical reactions involving NO_X that produce nitric acid and nitrate compounds. Anthropogenically emitted NOx undergoes photochemical oxidation with sunlight and oxidants to form HNO_3. This reacts with atmospheric alkaline substances to form soluble nitrates, which are scavenged by precipitation. Based on the regional characteristics of Ningbo and Guangzhou, it can be inferred that Na^+ and Cl^- in precipitation at the study sites

originated predominantly from sea salt. Their extensive coastal zones facilitate sea salt aerosol transport from sea surface evaporation and wave breaking to land. The absence of large-scale salt industries in the study areas rules out significant anthropogenic contributions to these ions. NH_4^+ and Ca^{2+} were the most abundant cations at both locations. NH_4^+ is mainly derived from NH_3 emissions associated with agricultural production activities such as nitrogen fertilizer volatilization and livestock excreta decomposition and industrial processes such as chemical manufacturing, coking, and waste treatment. Ca^{2+} primarily originates from soil dust, road dust resuspension, and construction activities [35]. Rapid urbanization such as earth-moving and road paving in both cities resuspends calcium-rich dust into the atmosphere. These particles dissolve in precipitation to release Ca^{2+}.

This study uses the Piper diagram to analyze the data of water-soluble ions. The modified Piper diagram has been successfully employed to illustrate the distribution characteristics of water-soluble ions in atmospheric particulate matter [36]. The compositional characteristics of water-soluble ions in wet deposition at the urban and coastal sites in Ningbo are illustrated in Figure 5. The ionic species present at the two observation sites were similar; however, each exhibited distinct features attributable to their respective geographical locations. At the ZX site (urban), water-soluble ions in wet deposition were predominantly characterized as a mixed type with a primary tendency toward nitrate-dominated composition. The cationic composition was biased toward the NH_4^+ type, with the relative proportions of K^+ and Ca^{2+} exceeding those of Na^+ and Mg^{2+}. Sample data points in the diagram exhibited a divergent distribution from the center toward the [K^++Ca^{2+}] and [Na^++Mg^{2+}] regions, respectively. The anionic composition was dominated by NO_3^- and Cl^-. In consideration of the characteristics at the CX site (coastal), water-soluble ions in wet deposition at this location were predominantly characterized as a mixed type with a tendency toward chloride-dominated composition. It should be noted that this apparent discrepancy is due to spatial variability. Cl^- predominance only takes place at some specific site like coastal sites. The cationic components were biased toward both the K^+ and Ca^{2+} type and the Na^+ and Mg^{2+} type, with sample data points displaying a divergent distribution from the center toward these two regions. The anionic composition was dominated by SO_4^{2-} and Cl^-, with a distinct bias toward the Cl^- type, reflecting marine influence characteristics.

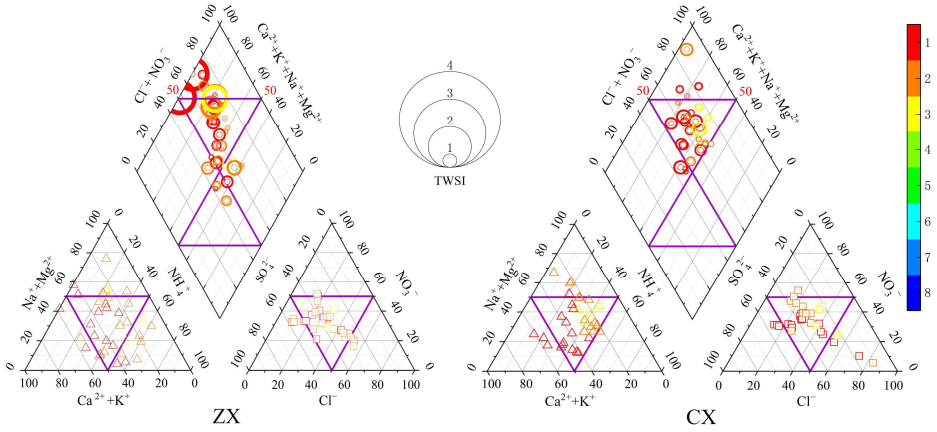

Figure 5. Modified Piper diagram for the characterization of the composition of water-soluble inorganic ions in Ningbo.

The compositional characteristics of water-soluble ions in wet deposition at the urban and coastal sites in Guangzhou are illustrated in Figure 6. The ionic species present at the two observation sites exhibited certain similarities while simultaneously reflecting distinct features associated with their respective geographical locations. At the GIG site

(urban), water-soluble ions in wet deposition were predominantly characterized as a mixed type with a tendency toward NH_4NO_3 and NH_4Cl dominance. The cationic composition was distinctly biased toward the NH_4^+ type, consistent with the urban location of GIG and suggesting the presence of traffic-related pollution risks in urban Guangzhou. The anionic composition was biased toward NO_3^- and SO_4^{2-}. At the WQS site (coastal), nitrate and chloride species in wet deposition exceeded sulfate, consistent with the marine characteristics of this sampling location. The cationic composition was biased toward both the Na^+ and Mg^{2+} type and the NH_4^+ type. The anionic composition was predominantly of the SO_4^{2-} type. Precipitation in the Guangzhou region continues to exhibit a risk of sulfuric acid-type acid rain, which warrants continued attention.

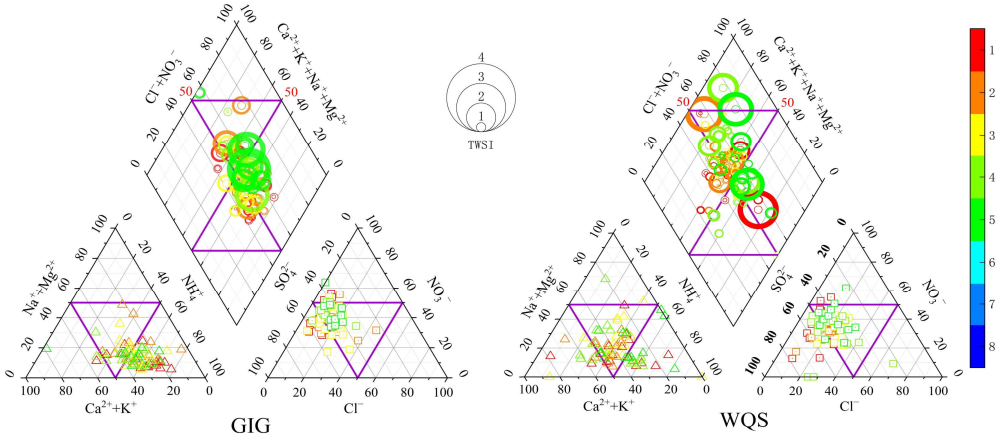

Figure 6. Modified Piper diagram for the characterization of the composition of water-soluble inorganic ions in Guangzhou.

3.4. The Water-Soluble Ionic Charge Balance

The anion–cation balance of the water-soluble ions analyzed in wet deposition samples from two sites in Ningbo and two sites in Guangzhou is illustrated in Figures S2 and S3, respectively. At the ZX and CX sites in Ningbo, the average CE/AE values were 1.06 and 0.96, respectively, indicating that the measured anion and cation concentration data are reliable. With R^2 = 0.93 and 0.88 ($p < 0.01$), the anions and cations examined in this study exhibited a good correlation, and the fitting effect was satisfactory. At the GIG and WQS sites in Guangzhou, the average CE/AE value was 1.10 and 1.07, respectively, demonstrating the reliability of the measured anion and cation concentration data. With R^2 = 0.92 and 0.77 ($p < 0.01$) confirmed a good correlation and satisfactory fitting effect, showing that the water-soluble anions and cations were generally balanced. Based on the above results, the analysis of water-soluble ion data at four sites is considered reliable.

3.5. Spatiotemporal Variations in Water-Soluble Ions in Atmospheric Wet Deposition

Figure 7 illustrates the temporal and spatial variations in the total concentrations of water-soluble ions in rainfall and the corresponding rainfall amounts at the urban (ZX) and coastal (CX) sites in Ningbo. The average monthly rainfall was 212 mm at the ZX site and 378 mm at the CX site. At both sites, SO_4^{2-} was the most abundant ion, with average concentrations of 68.02 μeq·L^{-1} at ZX and 58.76 μeq·L^{-1} at CX, while F^- exhibited the lowest concentrations, at 5.43 μeq·L^{-1} and 3.31 μeq·L^{-1}, respectively. Observations over three years in the Ningbo area indicate that the rainy season typically occurs in summer, while the dry season often occurs in late autumn and winter. A clear inverse relationship was observed between rainfall amount and the concentration of water-soluble ions, with concentrations being lower during periods of high rainfall and higher during periods of low rainfall. Research suggests that increased precipitation can dilute ion concentrations, and

that diffusion and evaporation also play significant roles [37]. The variation in water-soluble ion concentrations is also influenced by anthropogenic, marine, and crustal sources [38]. The total concentration of water-soluble ions at the coastal (CX) site was generally lower than that at the urban (ZX) site throughout the observation period. This suggests that pollutant emissions and ambient concentrations in the urban area may be higher than those in the coastal area. The urban areas have great anthropogenic emission contributions, while coastal locations have favorable dispersion conditions, jointly leading to higher ion concentrations in urban areas than coastal areas.

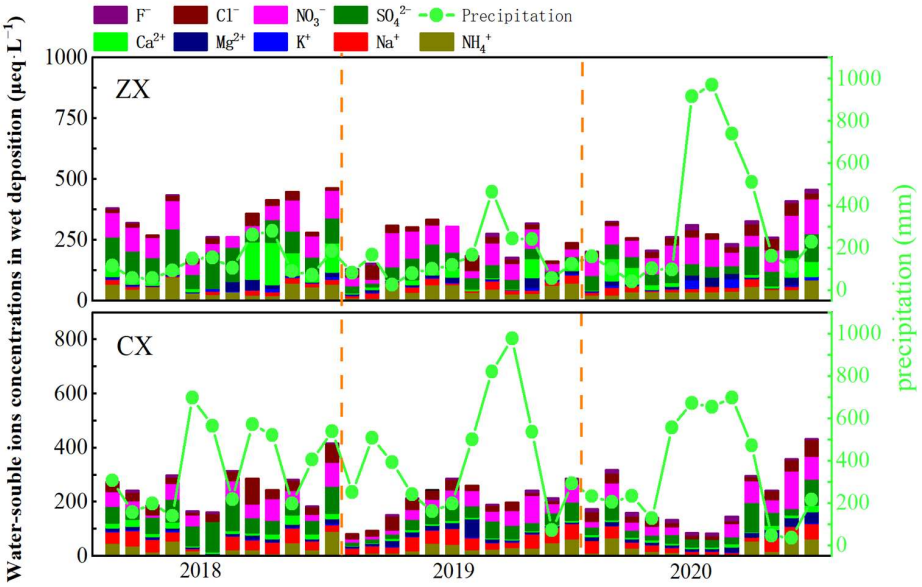

Figure 7. Temporal and spatial variation in water-soluble ion concentration in wet deposition in Ningbo.

Figure 8 illustrates the temporal and spatial variations in the total concentrations of water-soluble ions in rainfall and the corresponding rainfall amounts at the urban (GIG) and coastal (WQS) sites in Guangzhou. The average monthly rainfall was 172 mm at the GIG site and 425 mm at the WQS site. At both sites, SO_4^{2-} was the most abundant ion, with average concentrations of 117.03 μeq·L^{-1} at GIG and 102.64 μeq·L^{-1} at WQS, while K^+ exhibited the lowest concentrations, at 4.31 μeq·L^{-1} and 4.23 μeq·L^{-1}, respectively. The dry season extends from October to March of the following year, featuring low rainfall and relatively dry conditions. The rainy season occurs from April to September, characterized by high temperatures, abundant rainfall, and prevailing southeasterly winds originating from marine areas. The trends in total water-soluble ion concentrations in rainfall at both the GIG and WQS sites clearly indicate that total ion concentrations were significantly higher during the dry season compared to the rainy season. Furthermore, an inverse relationship was observed between rainfall amount and total ion concentration: concentrations were low during periods of high rainfall and high during periods of low rainfall. Peak rainfall amounts typically occurred in June and July, while minimum rainfall amounts were recorded in December. High ion concentrations were generally observed in November and December, whereas low ion concentrations were primarily concentrated in the rainy season months of July and August. The chemical composition of rainfall in the Guangzhou region exhibits pronounced seasonal and regional variations.

Figure 9 presents the Pearson correlation analysis between water-soluble ion concentrations in wet deposition and rainfall amount at the observation sites in Ningbo and Guangzhou. At the ZX site, the concentrations of NH_4^+, Na^+, K^+, Mg^{2+}, Ca^{2+}, SO_4^{2-}, NO_3^-, Cl^-, and F^- in wet deposition exhibited a significant negative correlation with rainfall amount ($p < 0.05$). At the CX site, significant negative correlations with rainfall

amount ($p < 0.05$) were observed for NH_4^+, K^+, Mg^{2+}, Ca^{2+}, SO_4^{2-}, NO_3^-, Cl^-, and F^-. At the GIG site, the concentrations of NH_4^+, Na^+, K^+, SO_4^{2-}, and Cl^- in wet deposition were significantly negatively correlated with rainfall amount ($p < 0.05$); other ions exhibited negative correlations that were not statistically significant. At the WQS site, the concentrations of all analyzed ions all showed significant negative correlations with rainfall amount ($p < 0.05$). These analyses further validate the conclusions drawn from Figures 7 and 8, confirming that the wet deposition concentrations of atmospheric water-soluble ions are influenced and exhibit a significant negative correlation with rainfall amount. Higher rainfall amounts dilute the concentrations of water-soluble ions in wet deposition, and conversely, lower rainfall amounts are associated with higher ion concentrations.

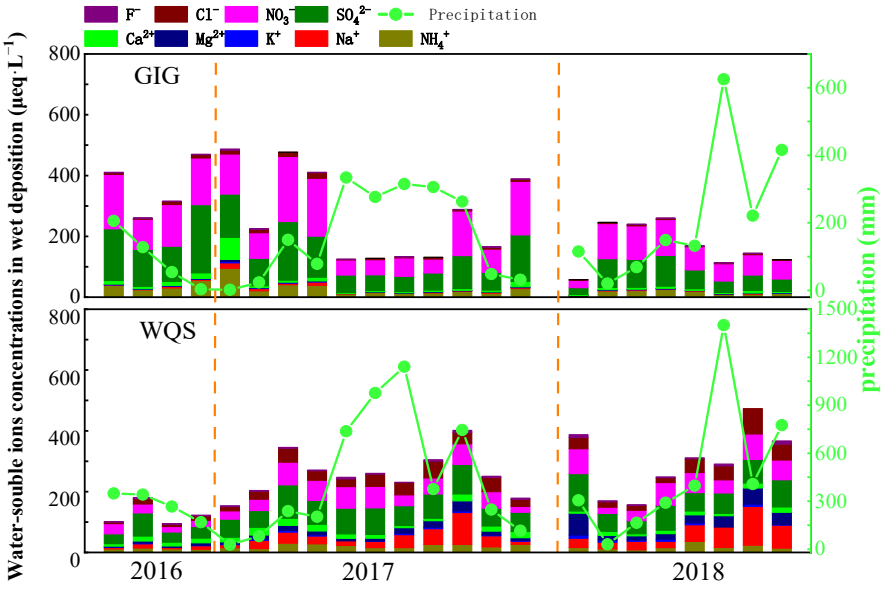

Figure 8. Temporal and spatial variation in water-soluble ion concentration in wet deposition in Guangzhou.

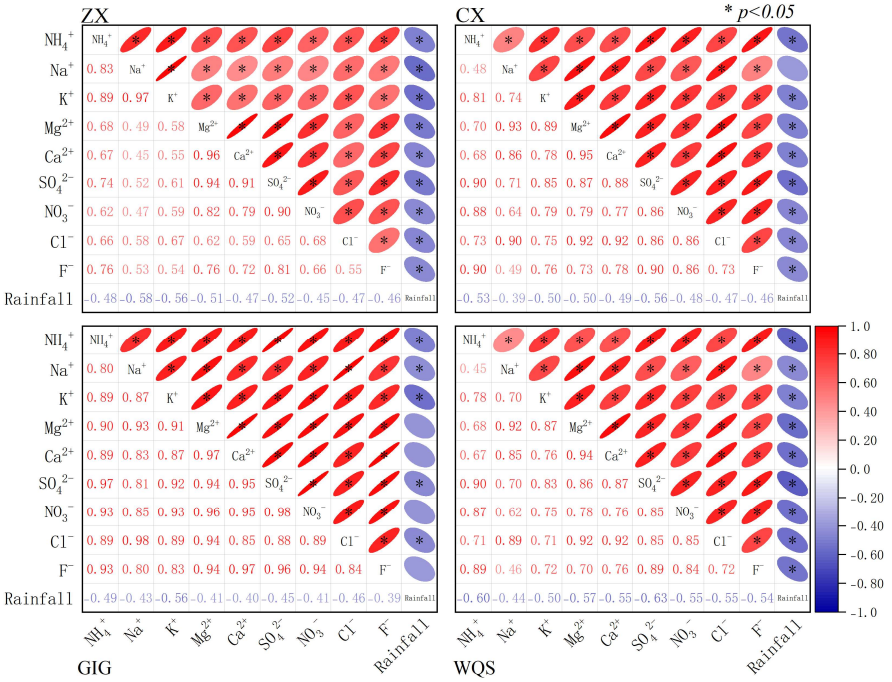

Figure 9. Pearson relationship between water-soluble ions concentration with rainfall in wet deposition in Ningbo and Guangzhou (* $p < 0.05$).

3.6. The Wet Deposition Flux of Water-Soluble Ions in the Atmosphere

The wet deposition fluxes of water-soluble ions in rainfall at the two Ningbo sites are presented in Figure 10. Overall, the highest fluxes of water-soluble ions in rainfall at both sites occurred primarily in summer, followed by autumn and winter, with the lowest fluxes observed in spring. The declining trend in ion fluxes over the study period suggests a gradual improvement in air quality. During the sampling period at both the ZX and CX sites, F^- exhibited the lowest deposition flux across all four seasons, ranging from 11 mg·m^{-2} to 23 mg·m^{-2}. The highest wet deposition flux at ZX occurred in summer from 4667 to 5156 mg·m^{-2}, while the lowest occurred in spring from 2667 to 2822 mg·m^{-2}. In contrast to the urban site CX, the lowest deposition flux at CX occurred in summer from 2753 to 2892 mg·m^{-2}, and the highest occurred in winter from 3389 to 3462 mg·m^{-2}. This difference may be attributable to the influence of the marine meteorological environment at the coastal site, where enhanced pollutant dispersion during summer reflects a pronounced marine influence.

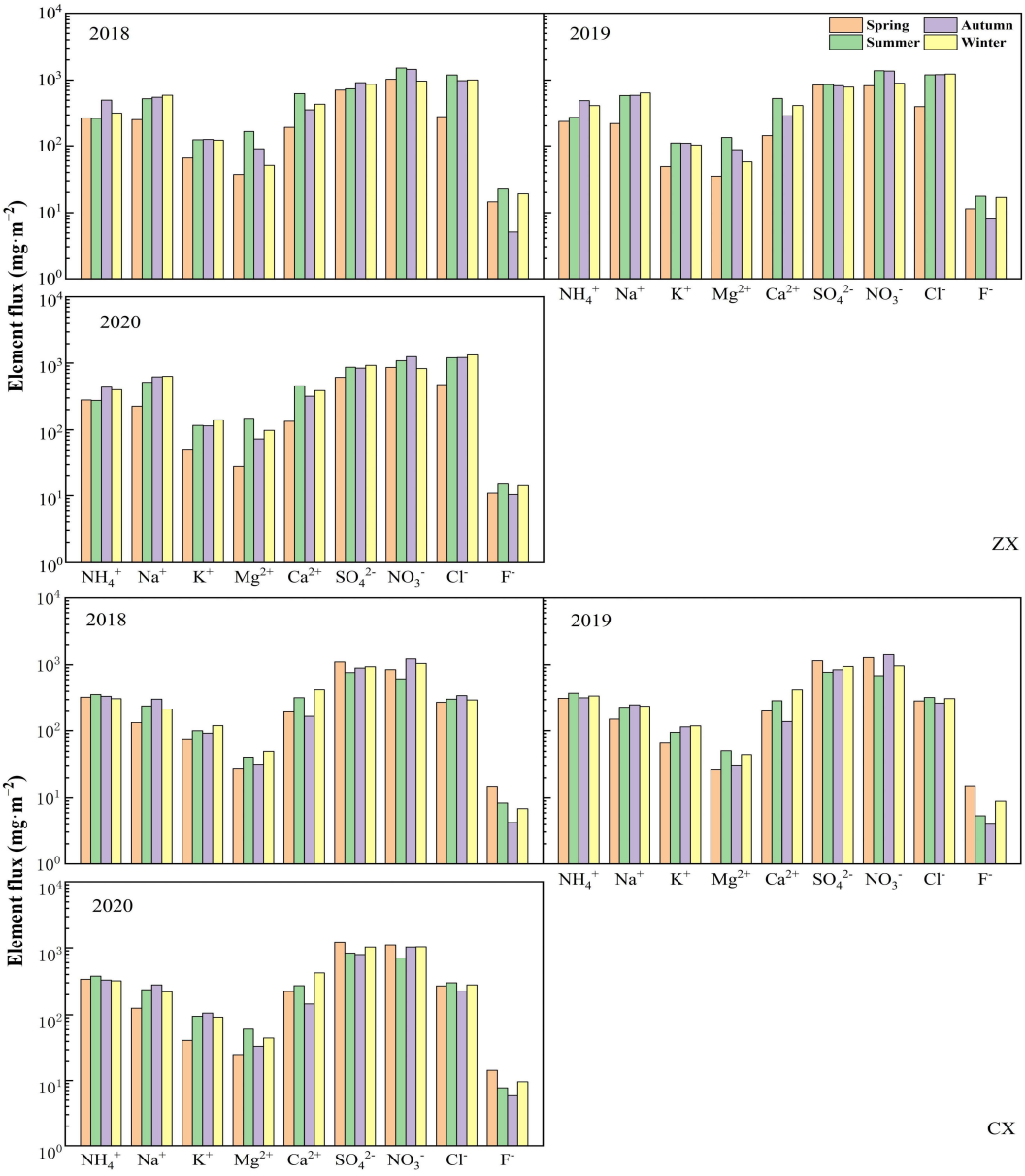

Figure 10. Spatial-temporal variation in water-soluble ion flux in wet deposition in Ningbo.

Figure 11 illustrates that the wet deposition fluxes of water-soluble ions in rainfall at the Guangzhou GIG and WQS sampling sites were primarily concentrated in the rainy season. At the GIG site, the difference in total ion deposition fluxes between the two sampling years was not pronounced. The ions with the lowest and highest deposition fluxes at GIG site were both F^- and NO_3^-, respectively. The deposition fluxes of NH_4^+, Mg^{2+}, Ca^{2+}, and F^- were notably higher in the rainy season than in the dry season, indicating that these ions were most effectively scavenged during the rainy season in this urban area. At the WQS site, the total ion deposition fluxes in 2017–2018 were generally slightly higher than those in 2016–2017. F^- and NO_3^- exhibited the lowest and highest fluxes over the two-year sampling period. The deposition fluxes of Na^+, Mg^{2+}, SO_4^{2-}, and Cl^- were significantly higher in the rainy season than in the dry season. This indicates that in regions with abundant rainfall, wet scavenging is more effective during the rainy season. In the Pearl River Delta region, the intensity of atmospheric convection is relatively weak during the dry season, which hinders the dispersion of atmospheric pollutants and leads to their gradual accumulation. Coupled with the low rainfall amount during the dry season, this results in lower wet deposition fluxes of water-soluble ions. Conversely, during the rainy season, strong atmospheric convection facilitates pollutant dispersion, and the high rainfall amount and frequency result in frequent scavenging of airborne pollutants. Consequently, wet deposition fluxes of water-soluble ions are higher during the rainy season. Based on the above analysis, it is evident that the deposition fluxes of various ions in rainfall exhibit significant differences across sampling locations and periods. Moreover, meteorological conditions play an important role in influencing ion deposition fluxes.

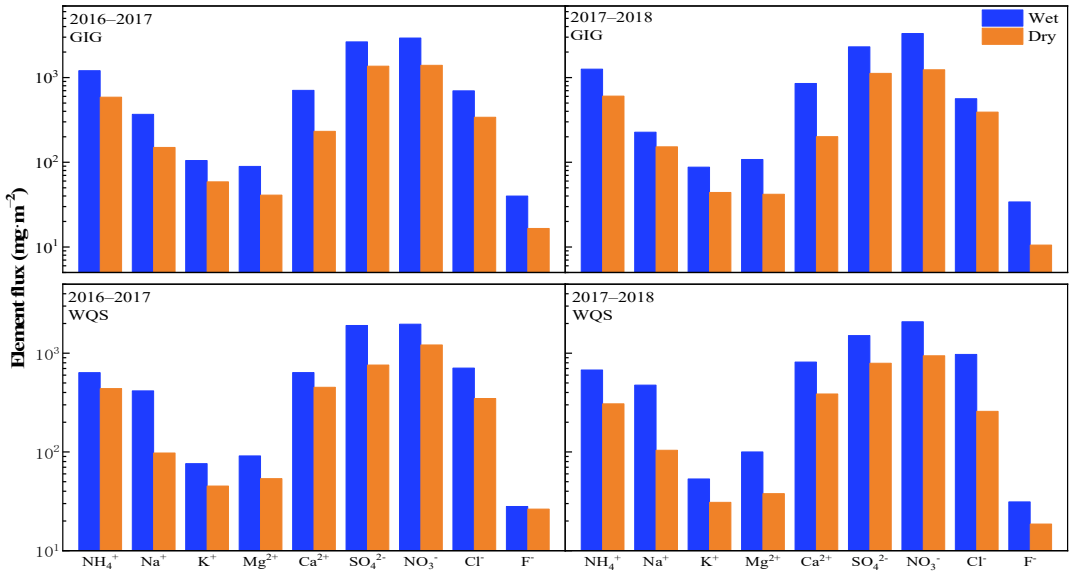

Figure 11. Spatial-temporal variation in water-soluble ion flux in wet deposition in Guangzhou.

3.7. Analysis of Ion Correlation in Atmospheric Wet Deposition

Table S3 presents the correlation analysis of water-soluble ions in precipitation samples collected at the ZX and CX sites in Ningbo. Strong correlations were observed among most ions. The correlation coefficients between SO_4^{2-} and NO_3^- were 0.89 at the ZX site and 0.84 at the CX site. These two ions are primarily derived from SO_2 and NO_X, respectively, indicating the homogeneity of atmospheric chemical components within the same region. Ca^{2+} and Mg^{2+} exhibited a high correlation coefficient of 0.96 and 0.94 at the ZX site and the CX site, respectively. It reflects the similar sources for Ca^{2+} and Mg^{2+}, predominantly associated with soil dust and road dust. The correlation coefficients between Cl^- and K^+, and between Cl^- and Mg^{2+}, were 0.66 and 0.61, respectively, at the ZX site, and 0.73

and 0.91, respectively, at the CX site. This indicates that atmospheric Cl^- in the Ningbo area primarily exists in the forms of KCl and $MgCl_2$. At the CX site, SO_4^{2-} and NO_3^- showed good correlations with both NH_4^+ and Ca^{2+}. This suggests that these ions in precipitation at the CX site mainly exist as $(NH_4)_2SO_4$, NH_4NO_3, $CaSO_4$, and $Ca(NO_3)_2$. In contrast, at the ZX site, Ca^{2+} exhibited strong correlations with SO_4^{2-} and NO_3^-, indicating that these ions in urban precipitation predominantly exist as $CaSO_4$ and $Ca(NO_3)_2$. The mass concentration ratio of NO_3^- to SO_4^{2-} in particulate matter can reflect the relative contributions of stationary and mobile sources to atmospheric sulfur and nitrogen. A NO_3^-/SO_4^{2-} ratio of less than 1 suggests that NO_3^- and SO_4^{2-} in atmospheric particles are primarily derived from stationary sources, whereas a ratio greater than 1 indicates a dominant contribution from mobile sources [39]. For instance, a ratio of 6.9 was observed in areas heavily impacted by vehicle exhaust, and the ratio of 0.9 was measured in regions with significant power plant emissions [40]. During the entire observation period, the NO_3^-/SO_4^{2-} ratio in wet deposition at the ZX site was 0.90, indicating that it is influenced by both mobile and stationary sources. The NO_3^-/SO_4^{2-} ratio in wet deposition at site CX was 0.70, indicating a greater contribution from stationary sources compared to site ZX. This is likely attributable to the industrial areas nearby the site CX. In contrast, the NO_3^-/SO_4^{2-} ratios observed in major Chinese cities, such as Shanghai (1.49) [41] was substantially higher, suggesting a more pronounced influence from mobile sources at the urban locations.

Table S4 presents the correlation analysis of water-soluble ions in rainfall samples collected at the GIG and WQS sites in Guangzhou from September 2016 to August 2018. At the GIG site, the correlation coefficients of NH_4^+ with SO_4^{2-} and NO_3^- were 0.95 and 0.76, respectively, while at the WQS site, they were 0.90 and 0.86, respectively. These strong correlations suggest that ammonium salts in the atmosphere primarily exist in the forms of ammonium sulfate and ammonium nitrate. Throughout the observation period, the NO_3^-/SO_4^{2-} ratio in wet deposition was 0.92 at the GIG site, indicating that this location is influenced by both mobile and stationary sources. At the WQS site, the NO_3^-/SO_4^{2-} ratio was 0.87, suggesting a predominant influence from stationary sources. The correlation coefficient between Ca^{2+} and Mg^{2+} was 0.87 at the GIG site, which was lower than the 0.91 observed at the coastal WQS site. These two elements share similar sources, primarily associated with soil dust and road dust. The higher correlation at the WQS site may be related to the extensive large-scale infrastructure activities that have persisted in the Nansha District in recent years. At the GIG site, the correlation coefficients of Cl^- with Na^+ and K^+ were 0.93 and 0.66, respectively, while at the WQS site, they were 0.96 and 0.59. This suggests that Cl^- primarily exists as NaCl in the atmosphere in Guangzhou.

4. Conclusions

Based on observations of water-soluble ions in rainfall at two representative cities, Ningbo and Guangzhou, this study analyzed the ion concentrations, spatiotemporal distribution patterns, and sources to further investigate the chemical characteristics of atmospheric precipitation in these two locations. The main conclusions are as follows:

At the Ningbo sites, the dominant ions were NO_3^- and SO_4^{2-}, accounting for 23.22% and 20.71% of the total ion equivalents at the ZX site, and 18.00% and 16.98% at the CX site, respectively. At the Guangzhou sites (GIG and WQS), the dominant ions in rainfall were SO_4^{2-}, NO_3^-, NH_4^+, and Ca^{2+}. At GIG, these ions constituted 23.29%, 21.42%, 20.37%, and 17.22% of the total, respectively. At WQS, their contributions were 20.60%, 17.95%, 20.13%, and 18.13%, respectively.

Most ions showed strong correlations indicating homogeneous atmospheric components or similar sources. The NO_3^-/SO_4^{2-} ratios all under 1 suggest stationary sources

dominated at all sites, with greater mobile source influence at urban sites than at coastal sites, and lower ratios than in major cities like Shanghai.

During the sampling period in Ningbo, the wet deposition fluxes of water-soluble ions at both sites were primarily concentrated in summer and autumn, followed by winter, with the lowest fluxes occurring in spring. At the urban Guangzhou site, the deposition fluxes of NH_4^+, Mg^{2+}, Ca^{2+}, and F^- were significantly higher in the rainy season than in the dry season, indicating more effective scavenging of these ions during the rainy season in the urban area. At the coastal Guangzhou site, the deposition fluxes of Na^+, Mg^{2+}, SO_4^{2-}, and Cl^- were significantly higher in the rainy season, suggesting greater scavenging efficiency for these marine-influenced ions during the wet period. This also demonstrates that in regions with abundant rainfall, wet scavenging is more effective during the rainy season. The observed declining trend in ion fluxes over the study period indirectly suggests a gradual improvement in air quality in the vicinity of the sampling sites.

Supplementary Materials: The following supporting information can be downloaded at: https://www.mdpi.com/article/10.3390/atmos17050495/s1, Table S1: Statistical data of water-soluble ion concentration in Ningbo wet deposition ($\mu eq \cdot L^{-1}$); Table S2: Statistical data of water-soluble ion concentration in Guangzhou wet deposition ($\mu eq \cdot L^{-1}$); Table S3: Correlation analysis of water-soluble ions in rainfall at ZX station and CX sites in Ningbo; Table S4: Correlation analysis of water-soluble ions in rainfall at GIG station and WQS sites in Guangzhou; Figure S1: Flow chart of the experimental design and analytical procedures; Figure S2: Charge balance of ions at ZX and CX sites in Ningbo; Figure S3: Charge balance of ions at GIG and WQS sites in Guangzhou.

Author Contributions: Writing—original draft preparation, investigation, methodology, Z.L. and D.L.; data curation, C.L.; writing—review and editing, resources, funding acquisition, C.H. and H.X. All authors have read and agreed to the published version of the manuscript.

Funding: This research was funded by the Zhejiang Natural Science Foundation (ZCLMS25B0702), and Ningbo Natural Science Foundation (No. 2023J303).

Institutional Review Board Statement: Not applicable.

Informed Consent Statement: Not applicable.

Data Availability Statement: The original contributions presented in this study are included in the article and the Supplementary Material. Further inquiries can be directed to the corresponding authors.

Acknowledgments: We would like to thank the editor and reviewers for their advice on this work.

Conflicts of Interest: Author Chunli Liu was employed by the company Yunnan Guoke Green Environmental Protection Co., Ltd. The remaining authors declare that the research was conducted in the absence of any commercial or financial relationships that could be construed as a potential conflict of interest.

References

1. He, X.; Zeng, J.; Wu, Q.; Ma, Q.; Zhang, J.; Fu, L.; Ge, X. Nitrogen-containing pollutant records in rainfall from the north-south boundary area in China: Compositions, variations, and sources. *Process Saf. Environ. Prot.* **2025**, *202*, 107759. [CrossRef]
2. Feng, W.; Guo, Z.; Peng, C.; Xiao, X.; Shi, L.; Zeng, P.; Ran, H.; Xue, Q. Atmospheric bulk deposition of heavy metal(loid)s in central south China: Fluxes, influencing factors and implication for paddy soils. *J. Hazard. Mater.* **2019**, *371*, 634–642. [CrossRef]
3. Cheng, I.; Al Mamun, A.; Zhang, L. A synthesis review on atmospheric wet deposition of particulate elements: Scavenging ratios, solubility, and flux measurements. *Environ. Rev.* **2021**, *29*, 340–353. [CrossRef]
4. Safi, Z.; Miyittah, M.; Offei, B.K.; Amenorpe, G. A systematic review of wet and dry deposition of reactive nitrogen, sulfur, and heavy metals: Ecosystem contamination and food chain disruption in Ghana. *Environ. Sci. Atmos.* **2025**, *5*, 756–784. [CrossRef]
5. Williamson, T.N.; Sena, K.L.; Shoda, M.E.; Barton, C.D. Four decades of regional wet deposition, local bulk deposition, and stream-water chemistry show the influence of nearby land use on forested streams in Central Appalachia. *J. Environ. Manag.* **2023**, *332*, 117392. [CrossRef] [PubMed]

6. Peng, X.; Fu, Y.; Zhang, G.; Sun, W.; Huang, J.; Guo, Z.; Lin, J.; Song, J.; Wang, X.; Peng, P.a.; et al. Wet Deposition of Black Carbon: Insights From a Comparative Study of Char/Soot in PM10 and Rainwater. *J. Geophys. Res. Atmos.* **2025**, *130*, e2024JD043095. [CrossRef]
7. Sricharoenvech, P.; Edwards, R.; Yaşar, M.; Gay, D.; Schauer, J.J. Investigation of Black Carbon Wet Deposition to the United States from National Atmospheric Deposition Network Samples. *Aerosol Air Qual. Res.* **2024**, *24*, 230089. [CrossRef]
8. Behera, S.N.; Betha, R.; Huang, X.; Balasubramanian, R. Characterization and estimation of human airway deposition of size-resolved particulate-bound trace elements during a recent haze episode in Southeast Asia. *Environ. Sci. Pollut. Res. Int.* **2015**, *22*, 4265–4280. [CrossRef]
9. Aas, W.; Shao, M.; Jin, L.; Larssen, T.; Zhao, D.; Xiang, R.; Zhang, J.; Xiao, J.; Duan, L. Air concentrations and wet deposition of major inorganic ions at five non-urban sites in China, 2001–2003. *Atmos. Environ.* **2007**, *41*, 1706–1716. [CrossRef]
10. Cao, Y.-Z.; Wang, S.; Zhang, G.; Luo, J.; Lu, S. Chemical characteristics of wet precipitation at an urban site of Guangzhou, South China. *Atmos. Res.* **2009**, *94*, 462–469. [CrossRef]
11. Roy, A.; Chatterjee, A.; Tiwari, S.; Sarkar, C.; Das, S.K.; Ghosh, S.K.; Raha, S. Precipitation chemistry over urban, rural and high altitude Himalayan stations in eastern India. *Atmos. Res.* **2016**, *181*, 44–53. [CrossRef]
12. Cerro, J.C.; Cerda, V.; Caballero, S.; Bujosa, C.; Alastuey, A.; Querol, X.; Pey, J. Chemistry of dry and wet atmospheric deposition over the Balearic Islands, NW Mediterranean: Source apportionment and African dust areas. *Sci. Total Environ.* **2020**, *747*, 141187. [CrossRef]
13. Wang, B.; Luo, X.; Liu, D.; Su, Y.; Wu, Z. The effect of construction dust and agricultural fertilization on the precipitation chemical composition during summer in the Yangtze River Delta area, China. *Atmos. Pollut. Res.* **2021**, *12*, 101121. [CrossRef]
14. Thériault, J.M.; Stewart, R.E.; Henson, W. Impacts of terminal velocity on the trajectory of winter precipitation types. *Atmos. Res.* **2012**, *116*, 116–129. [CrossRef]
15. Conrad-Rooney, E.; Gewirtzman, J.; Pappas, Y.; Pasquarella, V.J.; Hutyra, L.R.; Templer, P.H. Atmospheric wet deposition in urban and suburban sites across the United States. *Atmos. Environ.* **2023**, *305*, 119783. [CrossRef]
16. Conradie, E.H.; Van Zyl, P.G.; Pienaar, J.J.; Beukes, J.P.; Galy-Lacaux, C.; Venter, A.D.; Mkhatshwa, G.V. The chemical composition and fluxes of atmospheric wet deposition at four sites in South Africa. *Atmos. Environ.* **2016**, *146*, 113–131. [CrossRef]
17. Chen, Y.; Wang, Q.; Zhu, J.; Yang, M.; Hao, T.; Zhang, Q.; Xi, Y.; Yu, G. Multi-elemental stoichiometric ratios of atmospheric wet deposition in Chinese terrestrial ecosystems. *Environ. Res.* **2024**, *245*, 117987. [CrossRef]
18. Guo, T.; Li, M.; He, S.; Mo, Z.; Kang, X.; Pei, J.; Liao, W.; Chang, M.; Wang, X. Characterization of atmospheric arsenic wet deposition transport pathways and potential sources areas in the Pearl River Delta region. *J. Environ. Sci.* **2025**, *158*, 372–385. [CrossRef]
19. Zhao, X.; Sun, Y.; Zhao, C.; Jiang, H. Impact of Precipitation with Different Intensity on PM2.5 over Typical Regions of China. *Atmosphere* **2020**, *11*, 906. [CrossRef]
20. U.S. EPA. Method 3052: Microwave assisted acid digestion of siliceous and organically based matrices. In *Test Methods for Evaluating Solid Waste, Physical/Chemical Methods, SW-846*; U.S. EPA: Washington, DC, USA, 1996. Available online: https://www.epa.gov/sites/default/files/2015-12/documents/3052.pdf (accessed on 25 April 2026).
21. Li, T.; Wang, Z.; Wang, Y.; Wu, C.; Liang, Y.; Xia, M.; Yu, C.; Yun, H.; Wang, W.; Wang, Y.; et al. Chemical characteristics of cloud water and the impacts on aerosol properties at a subtropical mountain site in Hong Kong SAR. *Atmos. Chem. Phys.* **2020**, *20*, 391–407. [CrossRef]
22. Tao, J.; Wu, Y.; Deng, Y.; Hu, B.; Zhou, Z. Thermodynamic regulation of aerosol pH by temperature and humidity: The role of gas-particle partitioning of semi-volatile inorganic species in a subtropical region. *Environ. Res.* **2025**, *286*, 122727. [CrossRef]
23. Tu, J.; Wang, H.; Zhang, Z.; Jin, X.; Li, W. Trends in chemical composition of precipitation in Nanjing, China, during 1992–2003. *Atmos. Res.* **2005**, *73*, 283–298. [CrossRef]
24. Zhao, L.; Wang, X.; He, Q.; Wang, H.; Sheng, G.; Chan, L.Y.; Fu, J.; Blake, D.R. Exposure to hazardous volatile organic compounds, PM10 and CO while walking along streets in urban Guangzhou, China. *Atmos. Environ.* **2004**, *38*, 6177–6184. [CrossRef]
25. Zhang, Q.; Zhu, J.; Wang, Q.; Xu, L.; Li, M.; Li, Y.; Liu, C.; He, N. New Insights Into Multi-Component Atmospheric Wet Deposition Across China: A Multidimensional Analysis. *Earth's Future* **2022**, *10*, e2021EF002588. [CrossRef]
26. Liu, S. Synthesis and anion recognition of neutral receptors based on multiamide calixarene. *Sci. China Ser. B* **2004**, *47*, 648–653. [CrossRef]
27. Ma, M.; Wang, D.; Sun, R.; Shen, Y.; Huang, L. Gaseous mercury emissions from subtropical forested and open field soils in a national nature reserve, southwest China. *Atmos. Environ.* **2013**, *64*, 116–123. [CrossRef]
28. Geza, M.; Poeter, E.P.; McCray, J.E. Quantifying predictive uncertainty for a mountain-watershed model. *J. Hydrol.* **2009**, *376*, 170–181. [CrossRef]
29. Lin, C.; Huo, T.; Yang, F.; Wang, B.; Chen, Y.; Wang, H. Characteristics of Water-soluble Inorganic Ions in Aerosol and Precipitation and their Scavenging Ratios in an Urban Environment in Southwest China. *Aerosol Air Qual. Res.* **2021**, *21*, 200513. [CrossRef]

30. Shen, L.J.; Liu, C.Y.; Wang, H.L.; Diao, Y.W.; Shi, S.S.; Zhao, T.L. Changes of wet precipitation flux and pollutants associated with at Chongqing urban station from 2008 to 2020 and influencing factors. *J. Ecol. Rural. Environ.* **2024**, *40*, 1314–1322. [CrossRef]
31. Chen, Q.X.; He, Y.; Tang, Y.N.; Xu, Y.H.; Dai, M.T.; Huang, C.C.; Huang, T.; Yang, H. Chemical characteristics and source apportionment of atmospheric precipitation in Nanjing. *Acta Sci. Circumstantiae* **2024**, *44*, 112–123. [CrossRef]
32. Chu, P.C.; Chin, W.S.; Guo, Y.L.; Shiao, J.S. Long-Term Effects of Psychological Symptoms after Occupational Injury on Return to Work: A 6-Year Follow-Up. *Int. J. Environ. Res. Public Health* **2019**, *16*, 235. [CrossRef]
33. Feng, Y.; Zhao, S.; Wang, S.; Lin, Q.; Luo, Y.; Xu, S.; Yang, H.; Shi, J.; Zhang, M.; Jiao, L.; et al. Characteristics of Atmospheric Inorganic Nitrogen Wet Deposition in Coastal Urban Areas of Xiamen, China. *Atmosphere* **2021**, *12*, 1447. [CrossRef]
34. Feng, C.L.; Xing, J.W.; Yuan, H.M.; Song, J.M. Composition characteristics and source apportionment of water-soluble ions in atmospheric wet precipitation of Jiaozhou Bay. *Chin. J. Environ. Sci.* **2024**, *44*, 1225–1233.
35. Diana, A.; Bertinetti, S.; Abollino, O.; Giacomino, A.; Buoso, S.; Favilli, L.; Inaudi, P.; Malandrino, M. PM10 Element Distribution and Environmental-Sanitary Risk Analysis in Two Italian Industrial Cities. *Atmosphere* **2022**, *14*, 48. [CrossRef]
36. Yi, H.; Li, D.; Li, J.; Xu, L.; Huang, Z.; Xiao, H.; Tong, L. The Interrelated Pollution Characteristics of Atmospheric Speciated Mercury and Water-Soluble Inorganic Ions in Ningbo, China. *Atmosphere* **2023**, *14*, 1594. [CrossRef]
37. Shi, R.; Cooper, A.J.; Tanaka, H. Impact of Hierarchical Water Dipole Orderings on the Dynamics of Aqueous Salt Solutions. *Nat. Commun.* **2023**, *14*, 4613. [CrossRef]
38. Zhang, Z.; Li, C.; Deng, T.; He, J. Impacts of East Asian winter monsoon circulation on interannual variability of winter haze days in Guangdong Province. *Atmos. Res.* **2023**, *291*, 106793. [CrossRef]
39. Yao, X.; Chan, C.K.; Fang, M.; Cadle, S.; Chan, T.; Mulawa, P.; He, K.; Ye, B. The water-soluble ionic composition of PM2.5 in Shanghai and Beijing, China. *Atmos. Environ.* **2002**, *36*, 4223–4234. [CrossRef]
40. Tolocka, M.P.; Solomon, P.A.; Mitchell, W.; Norris, G.A.; Gemmill, D.B.; Wiener, R.W.; Vanderpool, R.W.; Homolya, J.B.; Rice, J. East versus West in the US: Chemical Characteristics of PM2.5during the Winter of 1999. *Aerosol Sci. Technol.* **2001**, *34*, 88–96. [CrossRef]
41. Chen, W.; Liu, X.-Y.; Yu, H.-Q. Temperature–dependent conformational variation of chromophoric dissolved organic matter and its consequent interaction with phenanthrene. *Environ. Pollut.* **2017**, *222*, 23–31. [CrossRef]